Integrated Multilayered Triboelectric Nanogenerator for Harvesting Biomechanical Energy from Human Motions

Peng Bai,[†,‡,#] Guang Zhu,[†,#] Zong-Hong Lin,[†] Qingshen Jing,[†] Jun Chen,[†] Gong Zhang,[‡] Jusheng Ma,[‡] and Zhong Lin Wang[†,§,*]

[†]School of Materials Science and Engineering, Georgia Institute of Technology, Atlanta, Georgia 30332-0245, United States, [‡]Department of Mechanical Engineering, Tsinghua University, Beijing10084, China, and [§]Beijing Institute of Nanoenergy and Nanosystems, Chinese Academy of Sciences, China. [#]P. Bai and G. Zhu contributed equally.

ABSTRACT We demonstrate a new flexible multilayered triboelectric nanogenerator (TENG) with extremely low cost, simple structure, small size (3.8 cm × 3.8 cm × 0.95 cm) and lightweight (7 g) by innovatively integrating five layers of units on a single flexible substrate. Owing to the unique structure and nanopore-based surface modification on the metal surface, the instantaneous short-circuit current (I_{sc}) and the open-circuit voltage (V_{oc}) could reach 0.66 mA and 215 V with an instantaneous maximum power density of 9.8 mW/cm^2 and 10.24 mW/cm^3. This is the first 3D integrated TENG for enhancing the output power. Triggered by press from normal walking, the TENG attached onto a shoe pad was able to instantaneously drive multiple commercial LED bulbs. With the flexible structure, the TENG can be further integrated into clothes or even attached onto human body without introducing sensible obstruction and discomfort to human motions. The novel design of TENG demonstrated here can be applied to potentially achieve self-powered portable electronics.

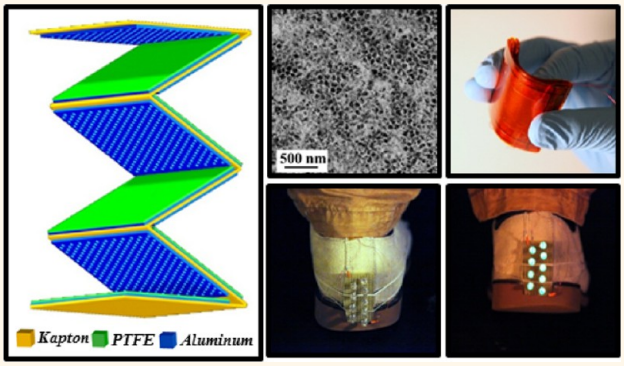

KEYWORDS: triboelectric nanogenerators · biomechanical energy · nanopores

Owing to enormous quantity and huge availability, diverse forms of ambient mechanical energy can be attractive sources for energy harvesting.[1−4] The mechanical energy harvesting techniques based on piezoelectric,[5−7] electrostatic,[8] and electromagnetic[9,10] mechanisms have been developed for applications in wireless sensing systems,[11] environment monitoring,[12,13] biomedicine,[14] and electronic devices.[15,16] As one of the most common forms of mechanical energy in our living environment, biomechanical energy generated by human motions such as walking is usually wasted.[17] If such form of mechanical energy can be effectively harvested, it will at least offset or even one day replace the reliance of our daily used portable electronic devices on traditional power supplies, such as batteries.[16] To accommodate the needs of harvesting energy from human motions, the generator is required to be small-sized, light-weighted, and flexible as well.

Recently, triboelectric nanogenerators (TENGs) have been demonstrated to be a powerful means of harvesting ambient mechanical energy based on triboelectric effect coupled with electrostatic effect.[18−20] Periodic contact and separation between two different materials that have opposite triboelectric polarities yields alternative flows of inductive free electrons between the electrodes.[21,22] However, previously demonstrated TENGs only had a single layer, making it challenging to substantially scale up the area density of the output power. Therefore, enhancing the output power inevitably involved largely increased area of a TENG.[23] Here in this work, we demonstrate an innovative design of a TENG with multiple

* Address correspondence to zlwang@gatech.edu.

Received for review February 14, 2013 and accepted March 13, 2013.

Published online March 13, 2013
10.1021/nn4007708

© 2013 American Chemical Society

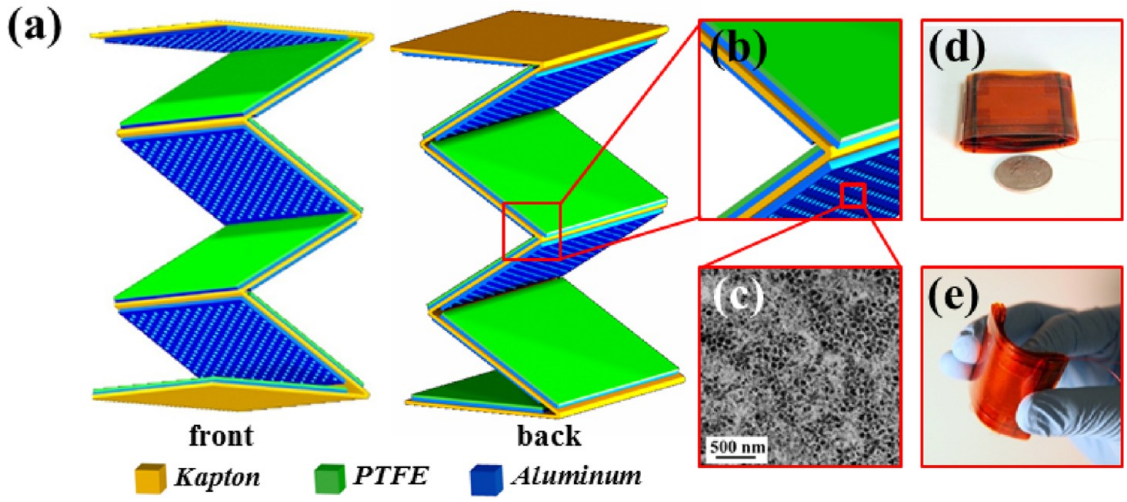

Figure 1. Structure and photographs of a flexible multilayered TENG with five layers of units. (a) Schematic and (b) an enlarged view of the zigzag-shaped structure of the TENG. (c) SEM image of nanopores on aluminum foils. (d) Photograph of a fabricated flexible multilayered TENG and (e) photograph of a bent flexible multilayered TENG by human fingers.

layers of units fabricated on a single flexible substrate. The structure provides a novel and simple method to stack multiple TENGs without either expanding the area or considerably complicating the fabrication process. As a consequence, we are able to achieve multifolds enhancement of the output power while keeping the TENG's area constant. A TENG with a size of 3.8 cm $\times$ 3.8 cm $\times$ 0.95 cm contains five active layers of units that are connected in parallel. The instantaneous short-circuit current (I_{sc}) and the open-circuit voltage (V_{oc}) could reach 0.66 mA and 215 V, corresponding to an instantaneous power density of 9.76 mW/cm^2 and 10.24 mW/cm^3 at device level. The light-weighted (7 g) and flexible TENG is extremely suitable for harvesting mechanical energy from human motions. Triggered by press from normal walking, the TENG attached onto a shoe pad was able to drive multiple commercial LED bulbs in real time. The innovative design of TENG demonstrated here can be further integrated into clothes or even attached onto human body to take the advantage of other human motions such as joint movements. It is expected to act as an effective supplementary power source for daily portable electronics.

RESULTS AND DISCUSSION

The structure of a flexible multilayered TENG from different views of angle is schemed in Figure 1a. A Kapton thin film with a thickness of 125 μm was selected as the substrate due to its availability, flexibility, lightweight, and proper stiffness. The Kapton film was shaped to a zigzag structure by making deformations at evenly spaced intervals (Figure 1b). The zigzag-shaped design enables that both sides of the Kapton film can serve as substrates of the TENG units. As sketched in Figure 1a, the TENG consists five layers of units, with three shown in the front view and the other two in the back view. For each layer, it incorporates an aluminum-coated polytetrafluoroethylene (PTFE) thin film and an aluminum foil with nanopore-based surface modification as the contact electrode. Figure 1c shows the distribution of the nanopores on the surface of aluminum foil. They play an important role in enhancing the output power, which will be discussed later. A thin film of aluminum was deposited on the back of PTFE as a back electrode. The whole TENG was packaged by fixing the deformed edges of the substrate together, as illustrated by a photograph of the as-fabricated TENG in Figure 1d. Further details of the fabrication process will be discussed in the Experimental Section. Demonstrated in Figure 1e, the fabricated TENG shows great flexibility, making it applicable to harvest energy not just from press but also from deformation.

The operating principle of the TENG can be described by the coupling of contact electrification and electrostatic induction. A layer of unit is selected to illustrate the energy conversion process (Figure 2). Without an applied force, a separation of the two plates is maintained owing to the stiffness of the substrate with an angle of θ_1 in Figure 2a. No charge transfer takes place, leading to no current flow. Under externally applied compressive force in the vertical direction, the PTFE film and the aluminum foil are brought into contact. According to the difference in triboelectric polarities,[24] surface triboelectric charges are generated through electrons transfer from aluminum to PTFE (Figure 2b). Once the compressive force is withdrawn, a separation forms as a result of stiffness of the substrate, producing an electric potential difference between the contact electrode and the back electrode.[15,23] Such a potential difference drives electrons from the back electrode to the contact electrode through an external circuit, screening the positive triboelectric charges on the

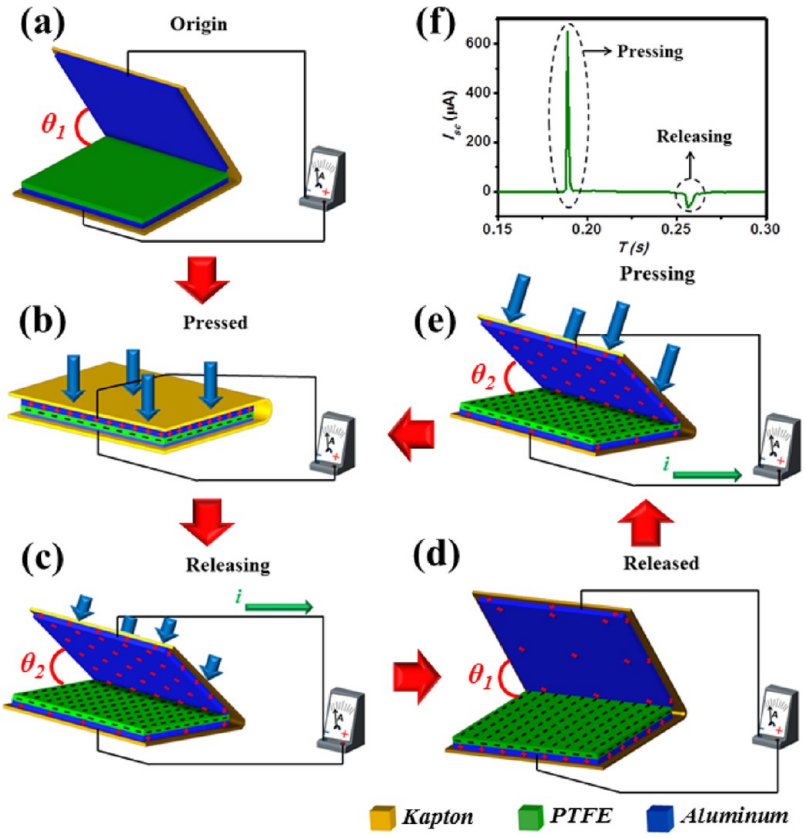

Figure 2. Working principle of the flexible multilayered TENG. (a) Original position with an angle of θ_1 between two plates. (b) External impact brings the PTFE thin film and the aluminum foil into contact, generating positive triboelectric charges on the aluminum side and negative charges on the PTFE side. (c) Withdrawal of the force causes a separation. Potential difference drives electrons from the back electrode to the contact electrode, screening the triboelectric charges and leaving behind inductive charges. (d) Two plates revert from the angle of θ_2 back to θ_1 with positive triboelectric charges almost entirely screened. (e) Electrons are driven back to the back electrode as the force is reapplied, reducing the positive inductive charges on the back electrode. (f) Short-circuit current of the TENG during one cycle. Note: For simplification, a layer of unit was shown and nanopores on the contact electrode are not shown in the schematics for simplicity of illustration.

contact electrode (Figure 2c). This process corresponds to an instantaneous negative current (Figure 2f). When the two plates revert to the fully released position, the positive triboelectric charges are almost totally neutralized by the inductive electrons (Figure 2d). It should be noted that negative triboelectric charges can still be retained on the surface of PTFE due to its insulating property.[25] When the compressive force is applied on the TENG again, a reversed potential difference is then produced to drive the inductive electrons to the back electrode in a reversed direction (Figure 2e), resulting in an instantaneous positive current (Figure 2f). After two plates get fully contacted again (Figure 2b), a cycle of electricity generation process is completed. It can be seen from Figure 2f that the current signal for pressing has a higher peak value but a shorter duration than that for releasing. It can be explained by the fact that the contact caused by external compressive force occurs more rapidly than the separation resulting from self-releasing of the substrate. Therefore, with a constant amount of inductive electrons transported back and forth between the electrodes, a quicker pressing corresponds to a larger output current.

Each layer fabricated on the zigzag-shaped substrate can be electrically connected with other layers in parallel through external wiring to enhance the output current. To characterize the output power of the multilayered TENG, a compressive contact force around 400 N generated from a human palm was applied (see Figure S1 in Supporting Information). Rectified I_{sc} values of individual layers were measured separately. Figure 3a displays the output current for each of these layers from the top to the bottom (Figure $3a_1-a_5$), respectively. It is noticed that the most top layer delivers the highest output current. It is suggested that this observation is attributed to the damping effect of the TENG's structure. The compressive force may be damped when it is transmitted from the top layer to the bottom layer. When all of the layers are put into parallel connection, an I_{sc} of 0.66 mA and a current density (J_{sc}) of 45.19 μA/cm^2 were achieved as shown in Figure $3a_6$. Likewise, we measured the V_{oc} of each layer (Figure $3b_1-3b_5$) and the TENG as a whole (Figure $3b_6$). The voltage of the entire TENG is not the sum of but comparable to the voltages from individual layers. The polarity of the measured electric signals

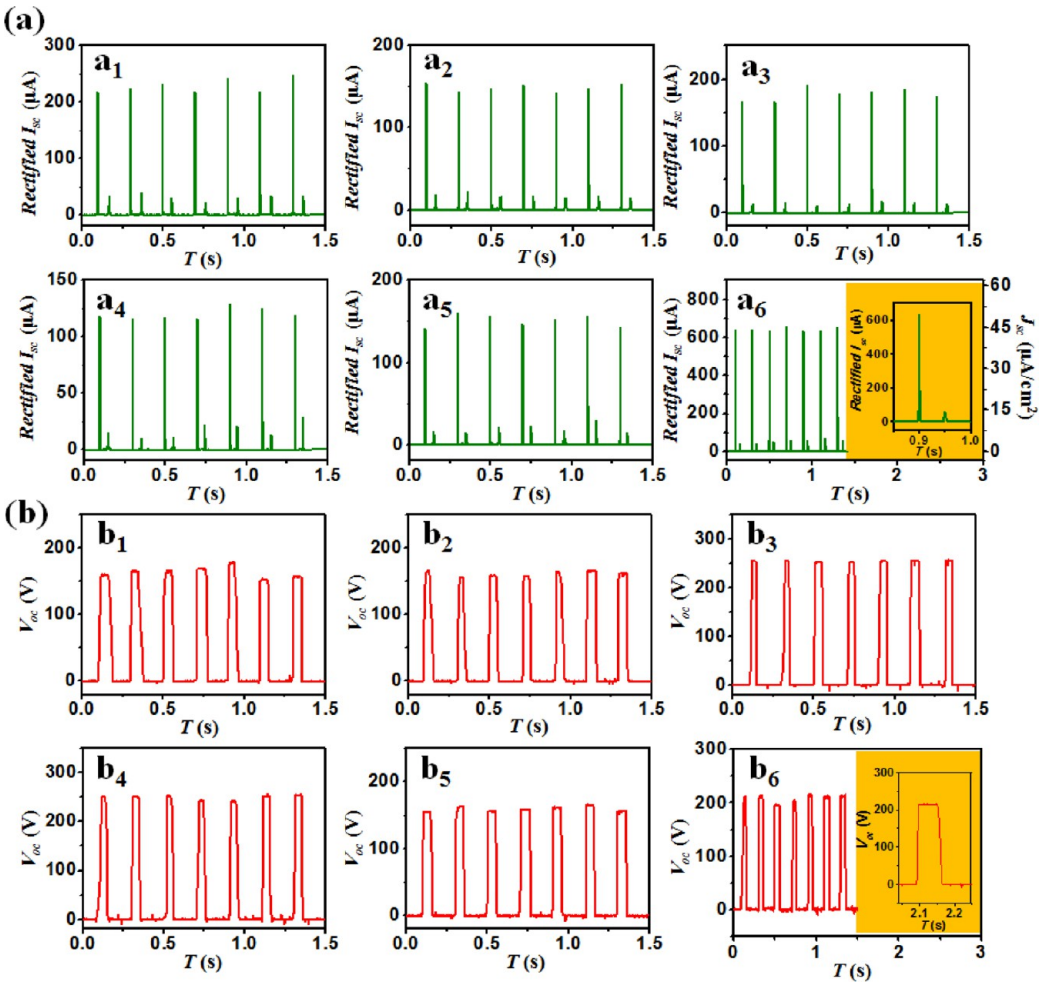

Figure 3. Output current and output voltage of the TENG with five layers of units. (a) Rectified short-circuit current (I_{sc}) under a contact force of 400 N applied by a human palm. Inset of panel a_6: enlarged view of one cycle, showing two current pulses in the same direction but contact corresponds to a larger current pulse. (b) Open-circuit voltage (V_{oc}) under contact force applied by a human palm. Inset of panel b_6: enlarged view of one cycle. Contact causes rising of the V_{oc} to a plateau value and separation makes it fall back to zero.

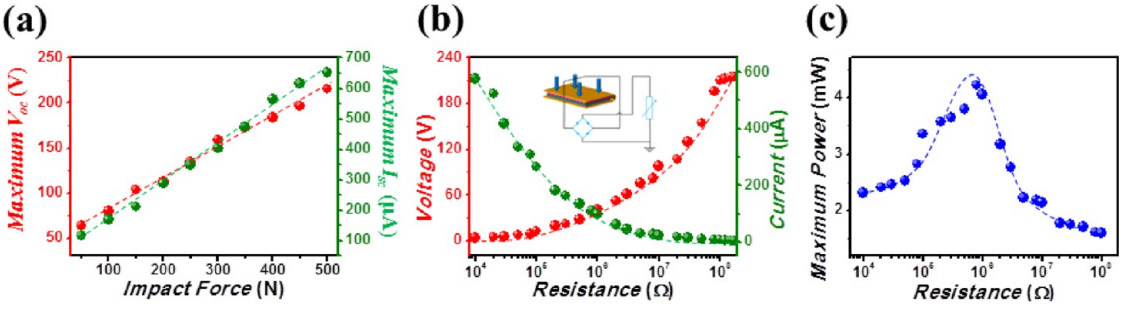

Figure 4. (a) Dependence of the I_{sc} and V_{oc} on the contact force. Larger contact force corresponds to higher current and voltage. The points represent peak value of electric signals while the lines are the fitted results. (b) Dependence of the output current on external load resistance under contact force applied by a human palm. Increased load resistance results in lower output current but higher output voltage. The points represent peak values of electric signals while the curves are fitted result. (c) Dependence of the output power on external load resistance under contact force applied by a human palm, indicating maximum output power when R = 1.0 MΩ. The curve is a fitted line.

above can be reversed by switching the connection polarity between the TENG and the measurement instrument (see Figure S2 and Figure S3 in Supporting Information). On the basis of the measurement results, it is effective to scale up the electric output by incorporating more layers on a longer substrate while keeping the area of the TENG constant.

The contact force is a critical factor that affects the TENG's electric output. As shown in Figure 4a, under a contact force of 50 N applied by a human palm,

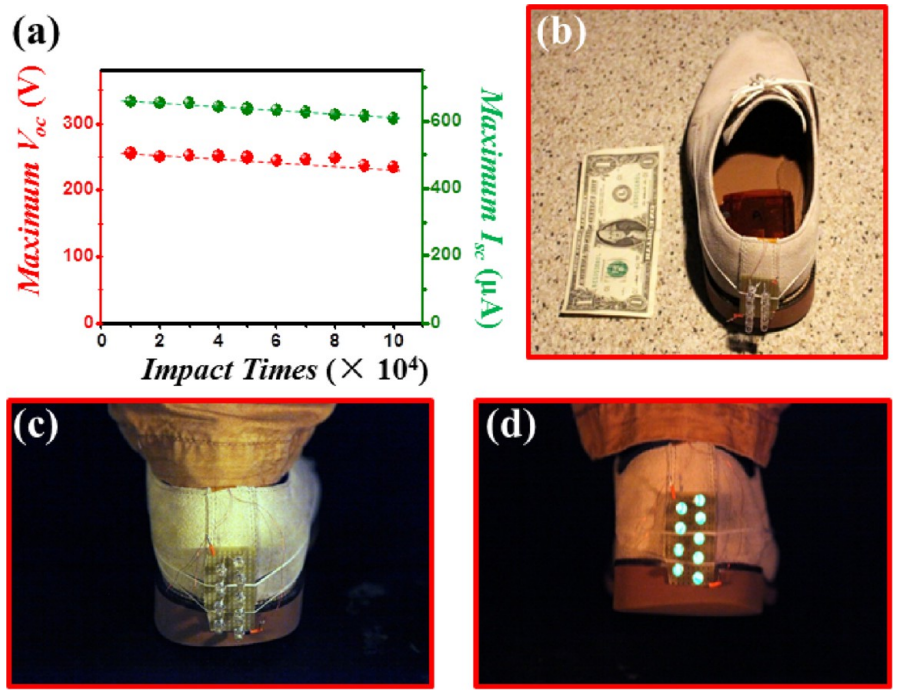

Figure 5. (a) Durability of the flexible multilayered TENG. The electric output remains stable although only a slight decline of the maximum I_{sc} and V_{oc} occurs. (b) Setup of the self-lighting shoe. (c) Photograph of the self-lighting shoe without foot motion. (b) Photograph of the self-lighting shoe during normal walking. Nine commercial LED bulbs were lit up simultaneously. Note: all LED bulbs were connected in series.

the maximum I_{sc} and V_{oc} generated by the TENG were 117 μA and 63 V, respectively. When the contact force increased to 500 N, the maximum I_{sc} of 656 μA and V_{oc} of 215 V were achieved. An approximate liner relationship between the contact force and the electric output can be derived from the results shown in Figure 4a. Larger contact force results in increased contact area and thus a larger amount of triboelectric charges. The enhanced contact area at larger contact force can be attributed to two probable reasons. First, the contact surfaces of the PTFE thin film and the aluminum foil are neither absolutely flat nor smooth. A larger contact force can reduce local gaps that may be introduced by surface roughness, substrate deformation, and contamination from the environment, leading to a larger contact area. In addition, nanopores on the aluminum foil play an important role in increasing the contact area. Under larger contact force, PTFE can deform and fill more vacant nanopores, further enhancing the contact area (see Figure S4 in Supporting Information). It is expected that the electric output would reach a saturated limit when all the nanopores are completely filled by PTFE.

In this work, resistors were used to investigate the reliance of the electric output power on the external load. As shown in Figure 4b, the maximum current decreased with increasing the resistance. On the contrary, the voltage across the load followed an opposite trend. Correspondingly, the instantaneous output power as a function of the resistance ($W = UI$) is displayed in Figured 4c. The maximum output power of 4.2 mW and a corresponding power density of 2.9 W/m^2 can be achieved at a load resistance of 1 MΩ. Such a power density can be further enhanced by more layers fabricated on the substrate. Moreover, the robustness of the TENG was investigated by using a mechanical shaker that generated impulsive impacts at a frequency of 10 Hz. Meanwhile, the I_{sc} and V_{oc} were measured for every ten thousands of the impacts. As shown in Figure 5a, only a slight decline (~7%) is observed for the maximum I_{sc} from 656 μA to 608 μA after a total of 100 000 impacts. Similarly, the maximum V_{oc} drops slightly from 215 to 195 V (~9%). The minor decrease of the electric output can be explained by the increased roughness of the PTFE thin film. A large number of impacts may lead to wrinkles on the PTFE thin film, reducing the total contact area between the aluminum foil and the PTFE thin film.

Here, a self-lighting shoe is developed, demonstrating the ability of the TENG to harvest biomechanical energy from human motions. The TENG was attached onto the shoe pad while a total of 9 commercial LED bulbs assembled in series on a piece of electric board were fixed at the back of the shoe (Figure 5b). Triggered by press from normal walking, the TENG directly and simultaneously powered all these LED bulbs (Figure 5c,d and the video in Supporting Information). The self-lighting shoe demonstrated here has immediate applications in indication, entertainment, and education. Owing to the small size, lightweight and flexibility of the TENG, it could be further integrated

into clothes or even directly attached to human body to harvest other human motions such as joint movements.

CONCLUSIONS

In summary, we demonstrated a novel structure of a flexible multilayered TENG by integrating five layers of units on a zigzag-shaped Kapton substrate. This innovative structure provides an effective means of scaling up the electric output of the TENG without increasing the TENG's area. The maximum power density of 9.76 mW/cm^2 and 10.24 mW/cm^3 (V_{oc} of 215 V and I_{sc} of 0.66 mA) were achieved. A self-lighting shoe has been demonstrated, which consists of a TENG attached onto the shoe pad and multiple LED bulbs fixed on the shoe surface. Driven by press from normal walking, the TENG was able to light up all of the LED bulbs simultaneously without introducing sensible discomfort to human motion. This study demonstrates the possibility of using the flexible multilayered TENG as an effective supplementary power source for portable electronics.

EXPERIMENTAL SECTION

Fabrication of a TENG with Five Layers of Units. A Kapton thin film (30.5 cm × 5.0 cm) with a thickness of 125 μm was used as the substrate. Five pieces of PTFE thin films were prepared and deposited with 100 nm of aluminum by e-beam evaporator. Then they were adhered onto the substrate with the uncoated side exposed. Subsequently, five pieces of aluminum foil with the same size as the PTFE films were adhered onto the substrate at corresponding positions. The five layers were connected in parallel by external wiring.

Nanopore-Based Surface Modification. The electrochemical anodization was applied on aluminum foil in 3% (mass fraction) oxalic acid ($H_2C_2O_4$) electrolyte. A platinum plate was used as the cathode. The aluminum foil was anodized under a bias voltage of 30 V for 5 h.[26,27] The alumina layer was etched away in a solution of 20 g/L chromic acid at 60 °C for 2 h. Then the aluminum foil was rinsed with DI water and dried in air.

Conflict of Interest: The authors declare no competing financial interest.

Acknowledgment. Research was supported by Airforce (MURI), U.S. Department of Energy, Office of Basic Energy Sciences (Award DE-FG02-07ER46394), NSF (0946418), and the Knowledge Innovation Program of the Chinese Academy of Science (Grant No. KJCX2-YW-M13). Peng Bai thanks the support from the Chinese Scholars Council. Patents have been filed based on the research results presented in this manuscript.

Supporting Information Available: (1) The contact force around 400 N measured by a force plate; (2) short-circuit current and reversed short-circuit current by switching the connection polarity between the TENG and the measurement instrument; (3) open-circuit voltage and reversed open-circuit voltage by switching the connection polarity between the TENG and the measurement instrument; (4) illustration of the force-dependence contact area. (5) supplementary video of a self-lighting shoe. This material is available free of charge *via* the Internet at http://pubs.acs.org.

REFERENCES AND NOTES

1. Wang, Z. L. Self-Powered Nanosensors and Nanosystems. *Adv. Mater.* **2011**, *24*, 280–285.
2. Paradiso, J. A.; Starner, T. Energy Scavenging for Mobile and Wireless Electronics. *IEEE Pervas. Comput.* **2005**, *4*, 18–27.
3. Xu, S.; Qin, Y.; Xu, C.; Wei, Y.; Wang, R.; Wang, Z. L. Self-Powered Nanowire Devices. *Nat. Nanotechnol.* **2010**, *5*, 366–373.
4. Dresslhaus, M. S.; Tomas, I. L. Alternative Energy Technologies. *Nature* **2001**, *414*, 332–337.
5. Wang, Z. L.; Song, J. H. Piezoelectric Nanogenerators Based on Zinc Oxide Nanowire Arrays. *Science* **2006**, *312*, 242–246.
6. Wang, X. D.; Song, J. H.; Liu, J.; Wang, Z. L. Direct-Current Nanogenerator Driven by Ultrasonic Waves. *Science* **2007**, *316*, 102–105.
7. Lee, S.; Hong, J. -I.; Xu, C.; Lee, M.; Kim, D.; Lin, L.; Hwang, W.; Wang, Z. L. Toward Robust Nanogenerator Using Aluminum Substrate. *Adv. Mater.* **2012**, *24*, 4398–4402.
8. Pelrine, R.; Kornbluh, R. D.; Eckerle, J.; Jeuck, P.; Oh, S.; Pei, Q.; Stanford, S. Dielectric Elastomers: Generator Mode Fundamentals and Applications. *Proc. SPIE* **2001**, *4329*, 148–156.
9. von Buren, T.; Mitcheson, P. D.; Green, T. C.; Yeatman, E. M.; Holmes, A. S.; Troster, G. Optimization of Inertial Micropower Generators for Human Walking Motion. *IEEE Sens. J.* **2006**, *6*, 28–38.
10. Williams, C. B.; Shearwood, C.; Harradine, M. A.; Mellor, P. H.; Birch, T. S.; Yates, R. B. Development of an Electromagnetic Micro-generator. *IEE Proc. Circuits, Dev., Syst.* **2001**, *148*, 337–342.
11. Beeby, S. P.; Tudor, M. J.; White, N. M. Energy Harvesting Vibration Sources for Microsystems Applications. *Meas. Sci. Technol.* **2006**, *17*, 175–195.
12. Lee, M.; Bae, J.; Lee, J.; Lee, C. -S.; Hong, S.; Wang, Z. L. Self-Powered Environmental Sensor System Driven by Nanogenerators. *Energy Environ. Sci.* **2011**, *4*, 3359–3363.
13. Lin, L.; Hu, Y.; Xu, C.; Zhang, Y.; Wen, X.; Wang, Z. L. Transparent Flexible Nanogenerator as Self-Powered Sensor for Transportation Monitoring. *Nano Energy* **2013**, *2*, 75–81.
14. Miao, P.; Mitcheson, P. D.; Holmes, A. S.; Yeatman, E. M.; Green, T. C.; Stark, B. H. MEMS Inertial Power Generators for Biomedical Applications. *Microsyst. Technol.* **2006**, *12*, 1079–1083.
15. Zhu, G.; Yang, R.; Wang, S.; Wang, Z. L. Flexible High-Output Nanogenerator Based on Lateral ZnO Nanowire Array. *Nano Lett.* **2010**, *10*, 3151–3155.
16. Hu, Y.; Lin, L.; Zhang, Y.; Wang, Z. L. Replacing a Battery by a Nanogenerator with 20 V Output. *Adv. Mater.* **2011**, *24*, 110–114.
17. Wang, Z. L. Self-Powered Nanotechnology. *Sci. Am.* **2008**, *298*, 82–87.
18. Fan, F. -R.; Tian, Z. -Q.; Wang, Z. L. Flexible Triboelectric Generator. *Nano Energy.* **2012**, *1*, 328–334.
19. Yang, Y.; Lin, L.; Zhang, Y.; Jing, Q.; Hou, T. -C.; Wang, Z. L. Self-Powered Magnetic Sensor Based on a Triboelectric Nanogenerator. *ACS Nano* **2012**, *6*, 10378–10383.
20. Fan, F. -R.; Lin, L.; Zhu, G.; Wu, W.; Zhang, R.; Wang, Z. L. Transparent Triboelectric Nanogenerators and Self-Powered Pressure Sensors Based on Micropatterned Plastic Films. *Nano Lett.* **2012**, *12*, 3109–3114.
21. Wang, S.; Lin, L.; Wang, Z. L. Nanoscale Triboelectric-Effect-Enabled Energy Conversion for Sustainably Powering Portable Electronics. *Nano Lett.* **2012**, *12*, 6339–6346.
22. Zhu, G.; Pan, C.; Guo, W.; Chen, C. -Y.; Yu, R.; Wang, Z. L. Triboelectric-Generator-Driven Pulse Electrodeposition for Micropatterning. *Nano Lett.* **2012**, *12*, 4960–4965.
23. Zhu, G.; Lin, Z. -H.; Jing, Q.; Bai, P.; Pan, C.; Yang, Y.; Zhou, Y.; Wang, Z. L. Toward Large-Scale Energy Harvesting by a Nanoparticle-Enhanced Triboelectric Nanogenerator. *Nano Lett.* **2013**, *13*, 847–853.
24. Nemeth, E.; Albrecht, V.; Schubert, G.; Simon, F. Polymer Tribo-electric Charging: Dependence on Thermodynamic Surface Properties and Relative Humidity. *J. Electrostat.* **2003**, *58*, 3–16.

25. Lowell, J.; Roseinnes, A. C. Contact Electrification. *Adv. Phys.* **1980**, *29*, 947–1023.
26. Thamida, S. K.; Chang, H. C. Nanoscale Pore Formation Dynamics during Aluminum Anodization. *Chaos* **2002**, *12*, 240–251.
27. Friedman, A. L.; Brittain, D.; Menon, L. Roles of pH and Acid Type in the Anodic Growth of Porous Alumina. *J. Chem. Phys.* **2007**, *127*, 154717.